Babeş-Bolyai University Cluj-Napoca
Faculty of Biology and Geology
Department of Experimental Biology

The Role of Brn3 Transcription Factors in Specification and Development of Neuronal Cell Types

Summary of the Doctoral Thesis

Scientific adviser
Acad. Prof. Dr. Octavian Popescu
PhD student
Szilárd Sajgó

Cluj-Napoca
2014

Contents

Key words

Cranial nerve
Brn3
cRet
Retinal Ganglion Cell
Expression profile
Viral infection

Introduction

Identifying functionally and morphologically distinct neuronal cell types can lead to a better understanding of neuronal circuits and ultimately the brain. The present thesis describes several methodological advances that can help decipher the molecular signatures of the developing brainstem and retinal ganglion cell neurons.

Brn3 transcription factors

Brn3a, Brn3b, Brn3c are members of the small subfamily of POU domain transcription factors (TF). The name POU is derived from three types of transcription factors, the pituitary-specific growth hormone regulating transcription factor (*Pit-1*), and the *Caenorhabditis elegans* specific octamer binding transcription factor *Oct-1* and the *Unc-86* [Herr et al., 1988]. *Brn3* transcription factors are expressed in retinal ganglion cells, inner ear hair cells, somatosensory, spiral and vestibular ganglia neurons [Badea and Nathans, 2011; Badea et al., 2012; Xiang et al., 1995]. The three different family members, *Brn3a Brn3b* and *Brn3c* are expressed in distinct morphological subtypes of retinal ganglion cells (RGC) and dorsal root ganglia neurons (DRG) [Badea and Nathans, 2011; Badea et al., 2012]. In the inner ear *Brn3a* and *Brn3b* are present in the spiral, and vestibular ganglion neurons, while *Brn3c* is the only one expressed in auditory and vestibular hair cells[Badea et al., 2012; Erkman et al., 1996; Gan et al., 1996; Ninkina et al., 1993; Turner et al., 1994; Xiang et al., 1997, 1995, 1998]. Targeted mutations of *Brn3* genes cause a large variety of phenotypes. *Brn3a* mutants die at birth. Other affected structures include loss of cells in the trigeminal ganglia (TGG), as well as follicle-associated sensory nerve endings. Retinal phenotype includes an increased ratio of bistratified cellular morphologies [Badea et al., 2009]. Deletion of *Brn3b* leads to 70% loss of retinal ganglion cells (RGC), [Erkman et al., 2000; Xiang et al., 1998], with the remaining cells exhibiting intra retinal axon guidance defects [Badea et al., 2009; Erkman et al., 2000].

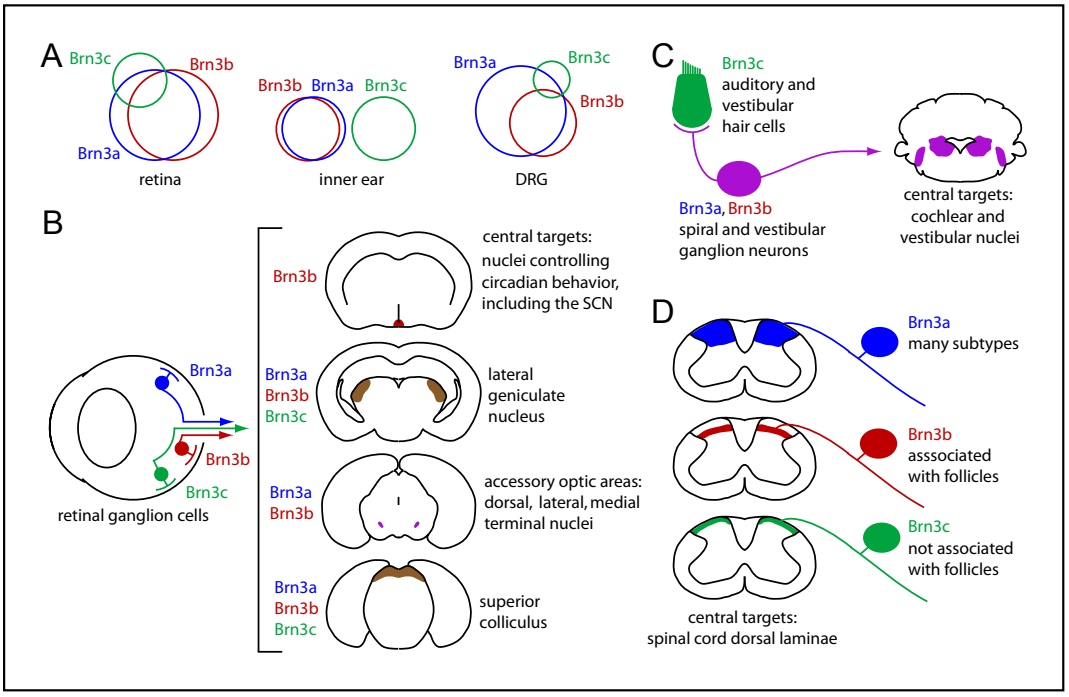

Figure 1: **Combinatorial expression of *Brn3*s.** (A) Diagrams representing the approximate numbers of neurons and their expression patterns of the three *Brn3* TFs in the retina inner ear and dorsal root ganglia (DRG). (B) Ganglion cells projecting to different CNS targets express different combinations of *Brn3a*, *Brn3b* and *Brn3c*. The circadion clock generator, suprachiasmatic nulceus (SCN) receives input only from *Brn3b+* RGCs. The lateral geniculate nucleus receives input from all three *Brn3* expressing cells, which relays it to the visual cortex. The accessory optic system controlling image stabilizing mechanisms receives input from *Brn3a* and *Brn3b* positive cells. The superior colliculus receives input from cells expressing *Brn3a*, *Brn3b* and *Brn3c*. (C) In the vestibulocochlear system, the sensory hair cells express *Brn3c*, and most spiral and vestibular ganglia express both *Brn3a* and *Brn3b*. (D) In the somatosensory system, *Brn3a* is expressed by all or nearly all classes of sensory neurons, while *Brn3b* is present in the follicle associated cells. *Brn3c* is expressed in non follicle associated fibers [Badea et al., 2012]

The Retina

The retina is an extension of the central nervous system, its major physiological function is to relay image-forming and non-image-forming [Foster and Hankins, 2002] visual information to the brain. Image forming vision consists of all visual information that is essential for object identification and tracking. Non-image-forming vision provides all the necessary cues for the synchronization of the biological clock with the dark-light cycle (circadian photoentrainment), controlling the pupil diameter and regulating many other biological behaviors [Fu et al., 2005]. The cellular diversity of the retina was first analyzed in detail 100 years ago by Cajal [Cajal, 1893]. Since Cajal it is known that the 200 µm thick tissue [Gollisch and Meister, 2010] at the back of the eye is composed of five different cellular classes, photoreceptors, bipolar, horizontal, amacrine and ganglion cells that are organized in three nuclear layers and two plexiform layers, where the synaptic wiring of these cells takes place [Masland, 2001] (see figure 2).

Retinal ganglion cells

Because the major focus of the present thesis is the retinal ganglion cell, its morphological and physiological characteristics will be discussed in more detail. Visual information gathered and processed by the retina is conveyed to the brain by 15-20 types of retinal ganglion cells [Badea and Nathans, 2011; Boycott and Wässle, 1974; Cajal, 1893; Masland, 2001; Wässle and Boycott, 1991; Wässle, 2004]. Retinal ganglion cell types can be identified based on their morphological properties [Amthor et al., 1984; Boycott and Wässle, 1974; Rockhill et al., 2002], like soma size [Oyster et al., 1981], dendritic lamination pattern and area. Based only on morphology the number of mouse retinal ganglion cell types varies: 11 [Badea and Nathans, 2004; Kong et al., 2005], 14 [Coombs et al., 2006], 17 [Sun et al., 2002], 22 [Völgyi et al., 2009]. By analyzing the morphology of a particular ganglion cell, it is possible to estimate its synaptic partners and to approximate its receptive field [Badea and Nathans, 2011; Kim et al., 2008].

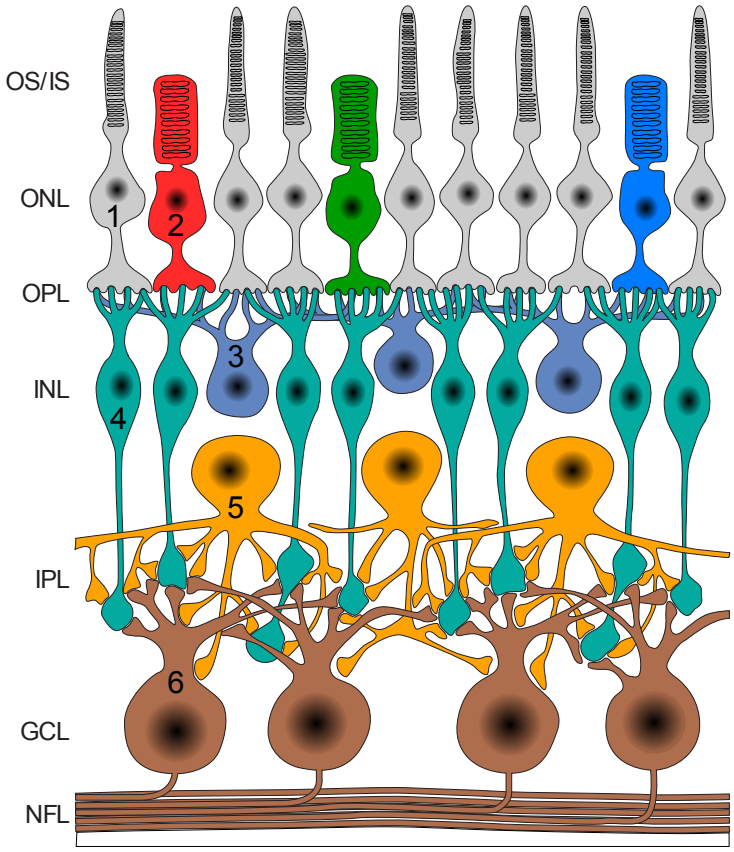

Figure 2: **Schematic of the mammalian retina.** The six classes of neuron in the mammalian retina: rods (1), cones (2), horizontal cells (3), bipolar cells (4), amacrine cells (5) and retinal ganglion cells (RGCs) (6). Their laminar distribution (OS/IS, outer and inner segments of rods, cones; ONL, outer nuclear layer; OPL, outer plexiform layer; INL, inner nuclear layer; IPL, inner plexiform layer; GCL, ganglion cell layer; NFL, optic nerve fiber layer) modified after [Wässle, 2004].

Objectives

The central nervous system is composed of millions of morphologically different interconnected neurons. Based on their function, neurons are divided into three main classes: sensory, motor and interneurons; each having multiple morphological and physiological variants. Distinct classes of neurons possess different molecular signatures conserved among different species. The primary aim of the present thesis is to identify which neuronal cell types of the developing nervous system express the neuron specific POU-domain transcription factor, Brn3b.

The mammalian retina contains approximately 50 morphologically different neurons Masland [2001]. The only projecting neuron of the retina is the retinal ganglion cell. The secondary aim of the thesis is to identify genes responsible for generating various morphologically and physiologically distinct retinal ganglion cells during development. For this purpose we analyzed the gene expression profiles of retinal ganglion cells by Next generation RNA sequencing. Aside from helping us decipher the regulators of neuronal diversity, this might also provide insight into disease mechanism, since many neurological disorders result from altered neuronal morphology.

The receptor tyrosine kinase, cRet, is expressed in trigeminal ganglia and in different types of dorsal root ganglia neurons. An additional aim of the present thesis is to study differential expression of cRet in various retinal ganglion cell types. cRet expressing ganglion cell morphologies were analyzed using sparse histochemical labeling.

The final objective of the thesis is to validate recently developed genetic tools for studying and manipulating neuronal circuits. Newly developed ganglion cell specific Cre expressing mouse lines will allow high resolution single cell analysis of developing RGCs.

Expression pattern of *Brn3b* during mouse development

To determine what other neuronal cell types involved in cranial nerve patterning express *Brn3b* in a constant or transient pattern, we analyzed embryonic tissues for *Brn3b* expression, by using a conditional Cre dependent $Brn3b^{CKOAP}$ reporter line [Badea et al., 2009]. In order to visualize the full expression pattern of *Brn3b* we used an ubiquitously expressed inducible CreER [Badea et al., 2003]. Activation of CreER was obtained by intraperitoneal injection of 4HT two days prior to embryo harvesting. In order to recombine the conditional *Brn3b* locus in a*Phox2b* dependent manner we used a *Phox2b* driven Cre [Scott et al., 2011].

Expression profile of *Brn3a* and *Brn3b* positive retinal ganglion cells

To determine the RNA expression profiles of *Brn3a* and *Brn3b* positive retinal ganglion cells at different developmental time points, *Brn3a* or *Brn3b* heterozygote animals containing an eye specific Cre, Pax6α-*Cre* (Figure **??**) [Marquardt et al., 2001] ($Brn3a^{WT/KO}$;Pax6α-*Cre* or $Brn3b^{WT/KO}$;Pax6α-*Cre*) were crossed to animals with homozygote $Brn3a^{CKOAP/CKOAP}$ or $Brn3b^{CKOAP/CKOAP}$ conditional alleles. The resulting offspring of this crossing is expected to be either $Brn3a^{AP/WT}$ or $Brn3a^{AP/KO}$ respectively $Brn3b^{AP/WT}$ or $Brn3b^{AP/KO}$ (see figure 3).

Retina harvested from E15.5 or P3.5 animals was dissociated using a papain-based protocol adapted from Tabata et al. [2000]. After tissue dissociation, retinal ganglion cells were separated from the cellular suspension by immunomagnetic purification. The protocol uses Pan Mouse IgG coated Dynal beads (Invitrogen, Carlsbad, CA, USA) coupled to an anti-AP mouse monoclonal antibody (VIB, Ghent, Belgium). Pre coating of the Dynal beads was performed in parallel with the tissue dissociation. The beads were incubated together with the anti-AP antibody for 40 min at RT.

Approximately 2×10^6 pre-coated Dynal beads were incubated with 10×10^6

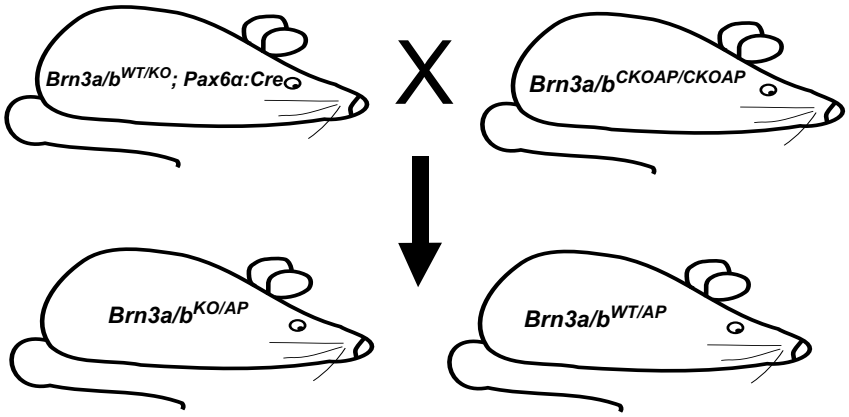

Figure 3: **Animal crosses.** Diagram showing performed crosses that result in animals having $Brn3a^{AP}$ and $Brn3b^{AP}$ positive retinal ganglion cells.

dissociated retinal cells for 5 min at RT. During incubation the glycosylphosphatidylinositol (GPI) anchored AP molecule is recognized and bound by the anti-AP coated Dynal beads. Following incubation the Dynal bead coupled AP positive ganglion cells were separated by magnetic isolation. After the donor animals were genotyped, 3-4 sorted samples were combined accordingly to increase RNA yield. Following RNA extraction was complete, expression profiles were analyzed by a Illumina Genome Analizer IIx.

A schematic of the various steps is depicted in figure 4.

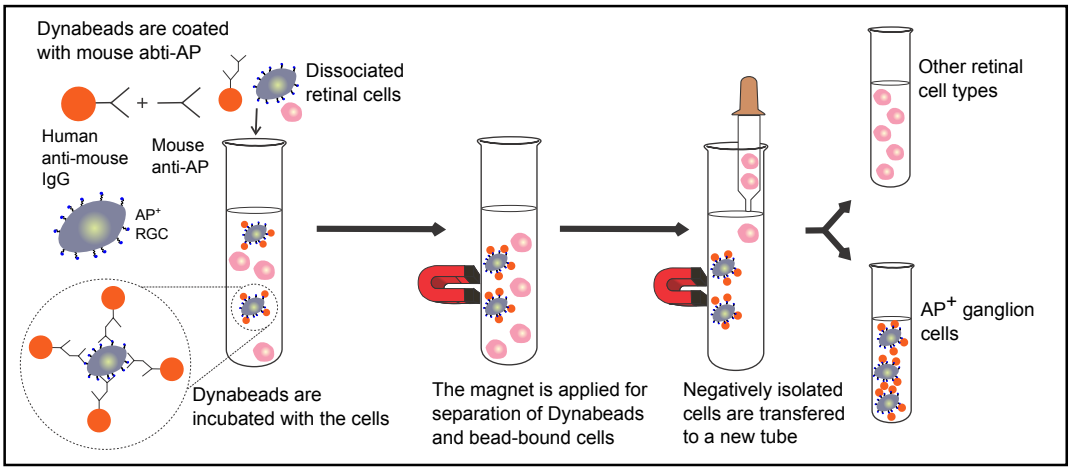

Figure 4: **Schematic of retinal ganglion cell sorting protocol.** Retinas containing *Brn3a/b*^{AP} positive ganglion cells were dissociated and incubated with Dynal bead coated with mouse anti-AP antibodies. Cells bound to Dynal beads were magnetically isolated. Adapted from Cat. no. 114.21D (Invitrogen Dynal AS Oslo)

In vivo functional analysis using viral vectors

Brn3a^{CKOCre} and *Brn3b*^{CKOCre} conditional Cre knock-in alleles

To enable in vivo functional analysis, Dre dependent conditional *Brn3a*^{CKOCre} and *Brn3b*^{CKOCre} mice were used, which were generated by Miruna Ghinia in collaboration with NIH-NEI Rodent Transgenic core facility. To demonstrate that the *Brn3a*^{Cre} and *Brn3b*^{Cre} alleles can successfully activate in a RGC dependent manner, a Cre dependent reporter virus, AAV1 - CAG - FLEX - tdTomato - WPRE - bGH (henceforth AAV1.FLEX.tdT) were used. For viral intraocular injection, postnatal day 0 (P0) pups were anesthetized by hypothermia in ice for 30 s, a slit was cut in the eye lid, and roughly 0.2 µL of a mix of two viral vectors including AAV1.FLEX.tdT (titer: $5.7 \cdot 10^8$), and AAV1.GFP (titer: $1 \cdot 10^8$) GFP virus, were injected, using a femtojet (Eppendorf) fitted with a pulled glass capillary. After the procedure, pups were placed on a heating pad and once fully recovered, they were returned to their mothers.

Expressionpattern of *Brn3b* during mouse development

In recent years molecular characterization of neuronal cell types has gained high importance. Visceral and somatic neurons can be distinguished based on their molecular signatures. Visceral neurons express and require the homeobox gene *Phox2b* Pattyn et al. [1997], somatomotor neurons express and require a combination of homeobox genes *Mnx1*, *Lhx3*, *Lhx4*, *Islet1* [Arber et al., 1999; Sharma et al., 1998; Tsuchida et al., 1994]. A vast majority of somatosensory neurons combinatorially express the POU domain related transcription factors *Brn3a*, *Brn3b* and *Brn3c* [Badea et al., 2012]. To determine what other neuronal cell types involved in cranial nerve patterning express *Brn3b* in a constant or transient pattern, we analyzed embryonic tissues for *Brn3b* expression, by using a conditional Cre dependent $Brn3b^{CKOAP}$ reporter line [Badea et al., 2009] (See figure5)

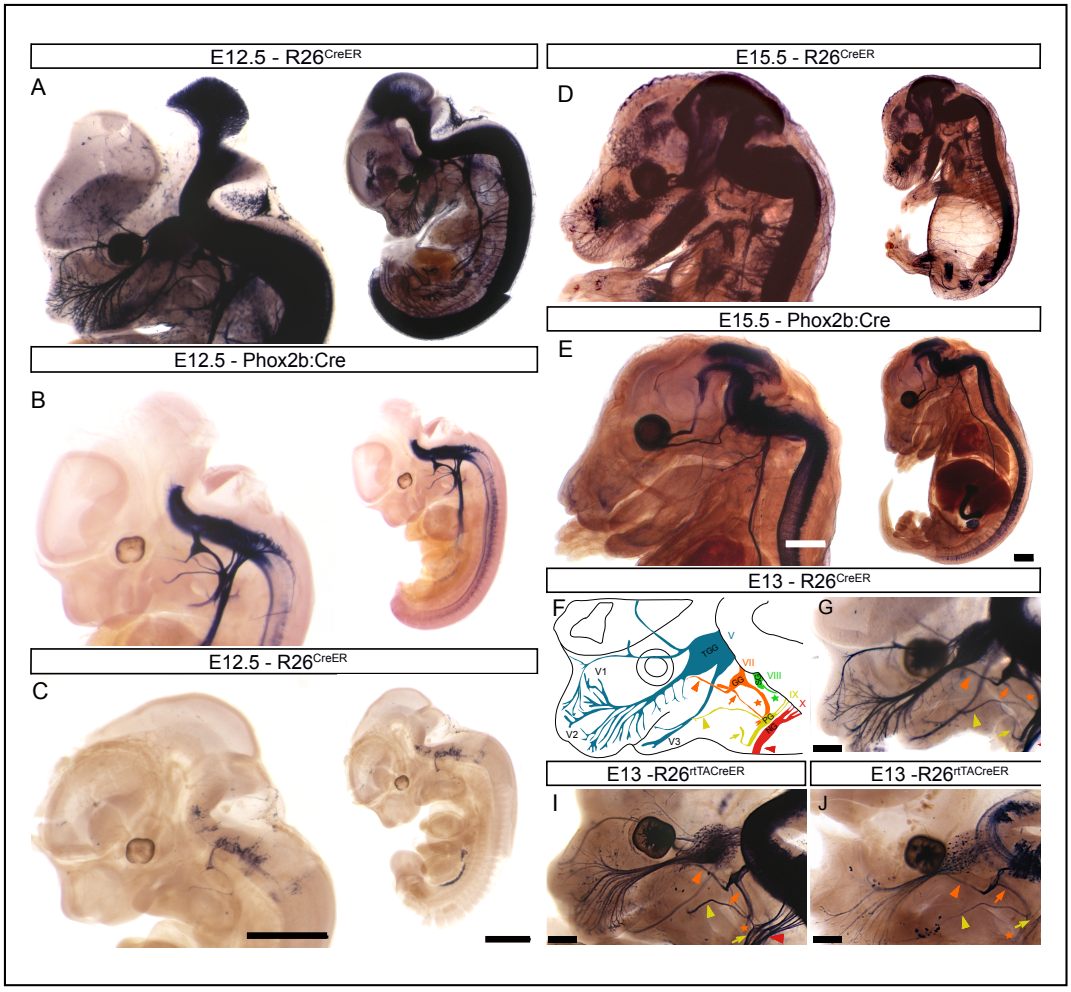

Figure 5: ***Brn3b* expression pattern during embryonic development.** To determine the embryonic pattern of *Brn3b* expression, $Brn3b^{CKOAP}$ conditional animals where crossed to (A,D,G) $R26^{CreER}$, (B,E) *Phox2b-Cre*, or (C,I,J) $R26^{rtTA\text{-}CreER}$ animals. Embryos where collected at days (A,B,C) 12.5, (G,I,J) 13 and (D,E) 15.5. Full expression pattern of *Brn3b* was determined by recombining the $Brn3b^{CKOAP}$ conditional allele using *CreER* expressed under the R26 promoter. (A,D,G) In order to saturate Cre activity, pregnant mothers were injected with 250 µg, of 4HT. AP positive regions included the retina, spinal cord, brainstem, mesencephalon, trigeminal ganglion (TGG), trigeminal nerve (V), facial (VII), glossopharyngeal (IX) and vagal nerves (X). (B,E) Intersection of *Brn3b* and *Phox2b* transcription factors was shown by recombining the *Brn3b* conditional allele with a *Phox2b* specific Cre. AP-expressing regions included the

spinal cord, nerves VII, IX and X. (C,I,J) Sparse expression pattern of *Brn3b* was obtained by using a $R26^{rtTA\text{-}CreER}$ line. The different levels of sparse recombination of the conditional allele was controlled by 0.2 mg/g Dox feed and (C) 12.5 µg, (I) 50 µg, (A,D,G) 250 µg, and (J) 17.5 µg4HT injections. (F-J) Detailed view of cranial nerves labeled at E13. (F) Detailed schematic of labeled nerves as seen by AP expression. Trigeminal nerve with its three branches: opthalmic (V1), maxillary (V2), mandibular (V3). Greater superficial petrosal (GSPN, orange arrow head), chorda tympani (CT, orange arrow), and main branches of the facial nerve (orange star). Vestibulocochlear nerve (green star), lingual (yellow arrowhead) and pharyngeal (yellow arrow) branches of the glossopharyngeal nerve and the nerve of the vagus (red arrowhead). (G-J) Different quantity of 4HT exposure allows the labeling of all or only a couple of nerve fibers in the developing cranial nerves. Scale bars: (A-E) 1 mm, (G-J) 500 µm.

Expressionprofile of *Brn3a* and *Brn3b* positive retinal ganglion cells

After basic validations, we started in-depth analysis of the expression profiles. All samples were processed in duplicate. For an overall comparison, duplicates as well as supernatant and RGC samples were plotted against each other, based on their expression value, reported in FPKM (see figure 6). A comparable number of transcripts were observed for both duplicates, and ganglion cell specific genes became evident (red circles figure 6). In total we have identified approximately 2500 genes that are enriched in the RGC samples versus the supernatant, (based on our two fold RGC enrichment versus retina, equal or greater than two FPKM criteria). Although the number of RGC specific genes is quite impressive, unfortunately the number of genes regulated by *Brn3a/b* was not evident at this resolution.

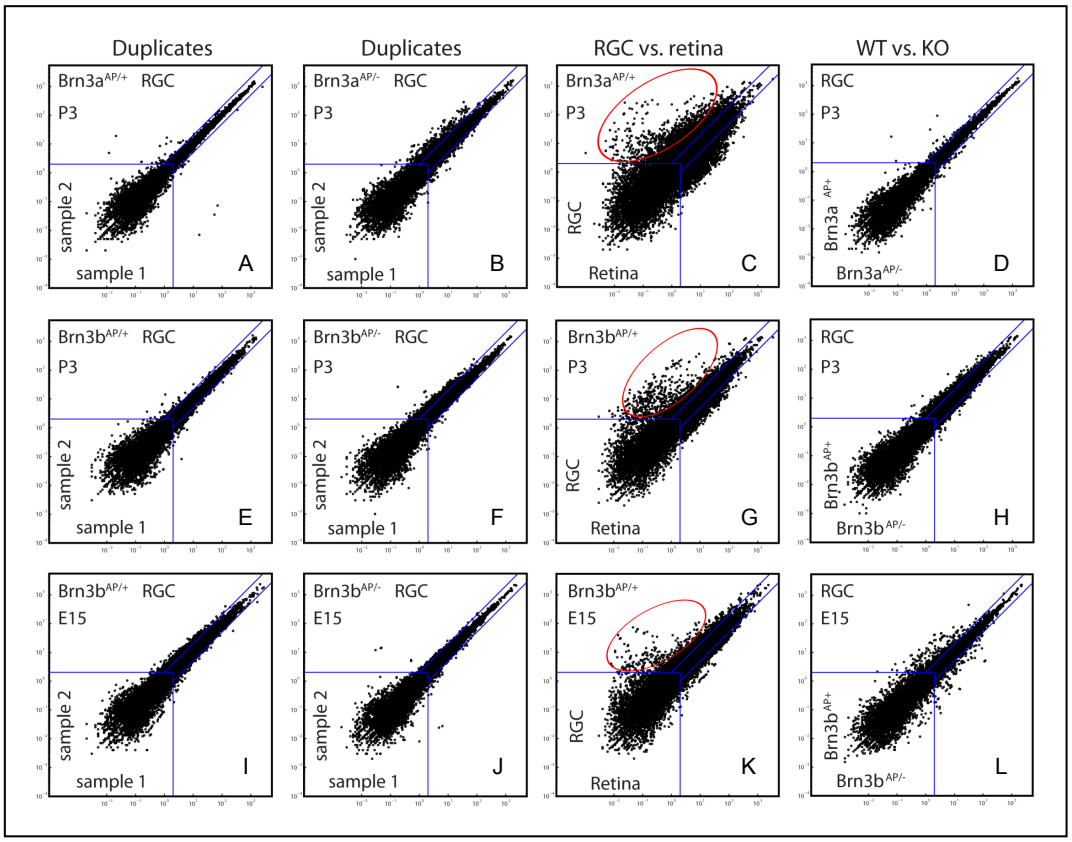

Figure 6: **Overall comparison of RNA Seq. samples.** The sequenced duplicates and RGC vs. supernatant samples plotted against each other. (A) *Brn3a*$^{AP/+}$, RGC sample1 vs. RGC sample2, P3, (B) *Brn3a*$^{AP/-}$, RGC sample1 vs. RGC sample2, P3, (C) *Brn3a*$^{AP/+}$, RGC vs. retina, P3, (D) *Brn3a*$^{AP/+}$ RGC vs. *Brn3a*$^{AP/-}$ RGC, P3, (E) *Brn3b*$^{AP/+}$, RGC sample1 vs. RGC sample2, P3, (F) *Brn3b*$^{AP/-}$, sample1 vs. sample2, P3, (G) *Brn3b*$^{AP/+}$, RGC vs. retina, P3, (H) *Brn3b*$^{AP/+}$ RGC vs. *Brn3b*$^{AP/-}$ RGC, P3, (I) *Brn3b*$^{AP/+}$, RGC sample1 vs. RGC sample2, E15, (J) *Brn3b*$^{AP/-}$, RGC sample1 vs. RGC sample2, E15, (K) *Brn3b*$^{AP/+}$, RGC vs. retina, E15, (L) *Brn3b*$^{AP/+}$ RGC vs. *Brn3b*$^{AP/-}$ RGC, E15. The threshold of 2 FPKM is marked by the blue lines. The blue diagonal lines reveal the twofold up or down regulation thresholds between samples represented on the X and Y axis. Red circles indicate RGC specific genes. Axes are FPKM in log scale.

Invivo functional analysis using viral vectors

The overall success of P0 eye injections was documented by the presence of GFP positive cells, which were infected by the Cre independent AAV1.CMV.GFP virus. Thus it can be easily appreciated from the green channel fluorescence of the retinal flat mounts that plenty of cells were infected in all retinas(figure 7). Finally, tdTomato positive cells were localized to the ganglion cell layer, and had characteristic axonal and dendrite arbor morphologies, indicative that these cells were RGCs.

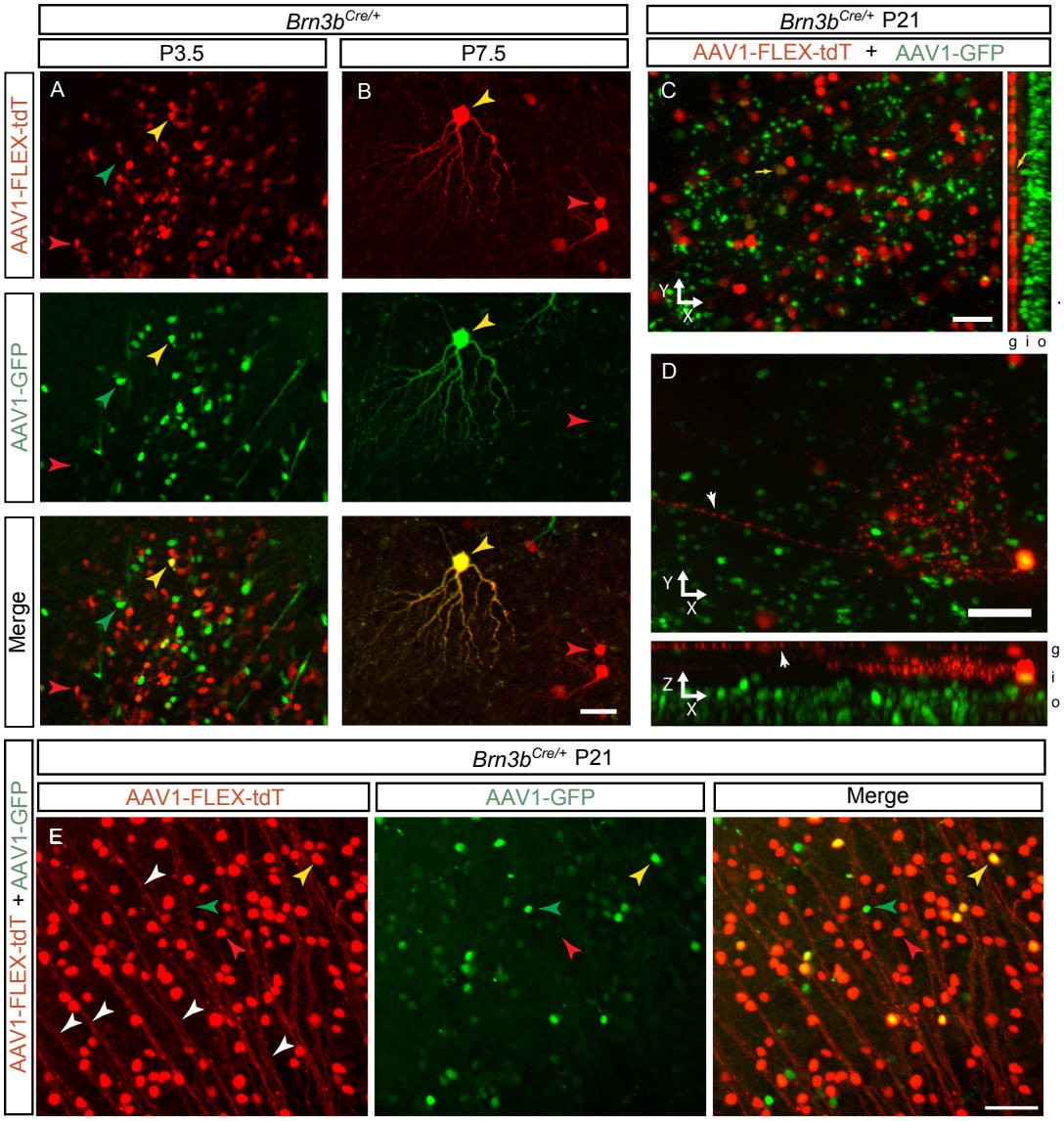

Figure 3.36: **AAV1-FLEX-tdTomato infection at P0 results in RGC specific tdTomato expression, which is already detectable at P3.5 and P7.5.** Retina samples are from (A) P3.5, (B) P7.5 pups or (C-E) adults. Panels in A, B are tdTomato (top), GFP (middle), and merged (bottom) images. Panels A-D are from *Brn3b*$^{Cre/+}$, and E from *Brn3a*$^{Cre/+}$ mice, infected at P0 after the protocol described in previous figure. Red, green and yellow arrowheads point at examples of red and green single positive or double positive cells. Note that the dendritic arbor of the double positive cell in B is clearly visible in both red and green channels. (C) Projections along the z direction (left) and x direction (right)

of a stack from a densely labeled *Brn3b*$^{Cre/+}$ retina, showing an overwhelming majority of red fluorescent cell bodies stratified in the GCL (g) layer, whereas abundant numbers of green fluorescent bodies are seen throughout the Inner and Outer Nuclear Layer (i and o). (D) Projections along the z direction (top) and y direction (bottom) of a stack from a sparsely infected *Brn3b*$^{Cre/+}$ retina showing a displaced RGC, with its axon (white arrowheads) and dendritic arbor, seen both from the flat mount and transversal perspective. (E) z projection of a stack from a densely labeled *Brn3a*$^{Cre/+}$ retina, showing single and double labeled cell bodies, and tdTomato labeled RGC axons (white arrowheads). Scale bars: 50 µm. Modified after [Sajgo et al., 2014].

Discussion

We have taken advantage of mouse lines developed by Badea et al. [2009], that conditionally activate AP expression from *Brn3a* or *Brn3b* promoters to visualize individual developing neurons of the brainstem, and to sort retinal ganglion cells for gene profiling. Therefore, the work described in my thesis will help determine what are the combinatorial genetic codes that determine neuronal fate. New technical developments in the field of gene profiling have led to the identification of several neuronal specific markers. Identification of these markers will be crucial to further understand neuronal communication and to allow for the genetic dissection of neural circuits. Several neuron specific markers like, *Brn3*, *Lhx*, *Phox2b*, *cRret* define morphologically and physiologically distinct cells types [Badea et al., 2012; Luo et al., 2009; Pattyn et al., 1997]. In the adult, expression patterns of these genes distinguish somatic *Brn3,Lhx,cRet* and visceral neurons *Phox2b+*. To investigate whether this is true for the developing nervous system we analyzed the expression patterns of *Brn3b*, *cRet* and *Phox2b* at diferent developmental time points. *Brn3b* expression was analyzed using genetically directed sparse labeling. This technique has several advantages over other labeling methods. Anterograde tracing by lipophilic dyes are only suitable for mass staining of projecting axons, while orescent labeling techniques are too weak to identify fine morphological details and Golgi staining is nonspecific. Using this labeling technique, we were able to further analyze Brn3 expression in the central and peripheral nervous system. We confirmed *Brn3b* expression in the trigeminal and geniculate sensory ganglia. This is not surprising since *Brn3b* is a known marker of somatosensory neurons [Badea et al., 2012]. The major relaying neurons of the retina, the ganglion cells (RGC) come in 20 different morphological variants. For precise analysis of RGC expression profiles we have taken advantage of mouse lines developed by Badea et al. [2009], that conditionally activate AP expression from *Brn3a* or *Brn3b* promoters, as described earlier. This allowed for RGC purification using anti-AP coupled Dynal beads. The specific aim of the screen was to identify genes responsible for the synthesis of large morphological variety during retinal development. By comparing the expression profiles of $Brn3a/b^{WT}$ and $Brn3a/b^{KO}$ retinal ganglion cells, we were able to gain insight into the molecular

mechanisms responsible for the mutant phenotypes seen in the knockout mice. *Brn3b* mutants lose 70% of their ganglion cells and show intraretinal axon guidance defects. Deletion of *Brn3a* has a milder retinal phenotype, increasing the number of bistratified RGCs